NUMERICAL SIMULATION OF PLATE HEAT EXCHANGER WITH IMPROVED MESH PERFORMANCE

Luan H.B.[a,b], Cao Z.[b] ,Wu Z.[b], Tao W.Q.[c] and Sunden B.[b,*]
*Author for correspondence
a. Research and Development Division, Shenhua Ningxia Coal Industry Group Co. Ltd, China
b. Department of Energy Science, Lund Unveristy, Lund, Sweden
c. School of Energy and Power Engineering, Xi'an Jiaotong University, Shaanxi, Xi'an, China
E-mail: bengt.sunden@energy.lth.se

ABSTRACT

A numerical and experimental study has been carried out on the heat transfer and fluid flow in a PHE. By means of a high-performance computing cluster, large-size and no-simplified plates can be simulated with 67 million computational cells. A new approach providing a proper clearance between two adjacent corrugated plates is proposed to improve the mesh quality around the contact points. The clearance value and the influence on the mesh quality and computational results are carefully studied. The results show that the ratio of clearance c to equivalent diameter D_e equals to 0.02 is proper. The CFD results agree with the experimental results with an error less than 10%. The proposed approach is proved to be effective and practical because it can increases the grid quality without losing the accurate of the results. This paper shows that CFD is a reliable tool for studying effect of various geometrical configurations on the optimum design of a PHE.

INTRODUCTION

Nowadays, the plate heat exchanger (PHEs) are widely used in many industrial applications [1]. With the rapid development of manufacturing technology, the welded plate heat exchanger can be applied in the temperature range from -200℃ to 900℃ and the pressure range is from full vacuum to 20MPa, which attracts more and more attention [2]. Computational fluid dynamics [3-5] (CFD) can be a useful tool for studying PHE in the following areas: thermal analysis, pressure drop, flow distribution, fouling and phase-change [6-11]. Extensive CFD works have been carried out on PHEs. The latest works are reported as follows.

Han et al.[7] investigated the temperature, pressure and flow distribution by CFD. When the fluid flows around the contact points, the speed and the direction will change dramatically. The physical models for the simulation were: the plate area A_p=0.2 m^2, the equivalent diameter D_e=7 mm and the computational cell number N_c=2.6 million.

Gherasim et al.[8] studied a 3D CFD model which considers more complex and realistic geometry of the distribution region. A comparison between experimental and numerical data has been conducted. The parameters were: the length of plate L_p=390 mm, the width of plate W_p=114 mm, D_e=7 mm, the mesh interval δ=0.6 mm and N_c=9.6 million.

NOMENCLATURE

A	[m^2]	Area
dp	[Pa]	Pressure drop
D	[m]	Diameter
h	[W/(m^{2}K)]	Heat transfer coefficient
j	[-]	Heat transfer factor
L	[m]	Length of plate
N	[-]	Number
Nu	[-]	Nusselt number
P	[mm]	Pitch of corrugation
Pr	[-]	Prandtl number
q	[-]	Mesh quality (aspect ratio for tetrahedron)
Q	[W]	Capacity
Re	[-]	Reynolds number
V	[m/s]	Velocity
W	[m]	Width of single plate
t	[m]	Clearance of two stacked plates
T	[K]	Temperature
x	[m]	Cartesian axis direction
y	[m]	Cartesian axis direction
z	[m]	Cartesian axis direction

Special characters

β	[°]	Inclination angle of two corrugations
δ	[mm]	Mesh interval
μ	[Pas]	Dynamic viscosity

Subscripts

c	Computational cell
e	Equivalent
p	Plate
w	Wall
in	Inlet

Tiwari et al.[9] analyzed the heat transfer and fluid flow in a PHE using nano-fluids. Validation of the CFD model suggests that considering the nano-fluid a homogeneous mixture, the simulations can be predicted reasonable accurate. The mesh information was: δ=0.5 mm, N_c=9.4 million.

Luan et al.[10] investigated the 3D geometry of PHE without simplification. The CFD results agree with the experiment result well. The parameters were: L_p=300 mm, W_p=300 mm, D_e=10 mm, δ=0.5 mm and N_c=27 million.

Giurgiu et al.[11] studied two types of heat exchangers with different geometry of the mini channel formed between two adjacent plates. The results obtained through numerical simulations showed that the PHE model using mini channel with inclination angle β=60 ° provided best heat transfer. The parameters of numerical model were L_p=40 mm, W_p =20 mm, D_e=1 mm and N_c=13.8 million.

In these simulations, there are a large number of contact points distributed in the corrugated PHE, which have a dramatically influence on the mesh quality around them. Grid generation is an important issue. It is required that a fine grid is employed where steep gradients appear. The computational cell number N_c is influenced by the ratio of D_eA/δ. Among all aforementioned works, it seems that work study on the mesh qualities and large-size computational cells with a high-performance cluster has not been tried out.

This paper proposes a new approach aimed to improve the mesh quality in PHE simulations. A proper clearance between two adjacent plates is provided to improve the mesh quality around the contact points. The value of clearance is studied and the effectiveness of the approach is verified. The paper is arranged as follows: section 2 describes the numerical model to be solved and gives an explanation of the new approach used in this work. Section 3 illustrates the results with different clearance values, the fluid flow and heat transfer results. Meanwhile, the validation of the CFD results with experimental result is also shown in this section. Finally, some conclusions are given in section 4.

NUMERICAL MODEL

Physical Model

The 3D geometry without any simplification is modeled by the software SOLIDWORKS shown in Figure 1a**.** The plate geometry considered here consists of several corrugations. The passage structure (Figure 1b) formed by two plates is very complicated. There exists many contact points and the passage patterns like a net.

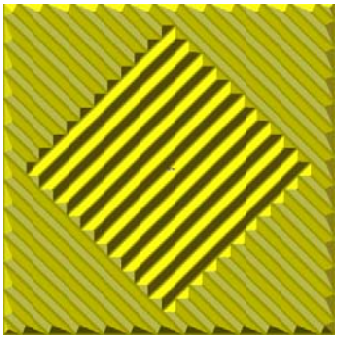

(a) Corrugated plate

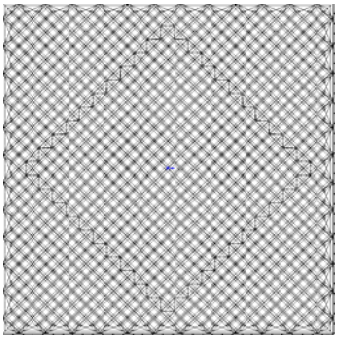

(b) Sketch of two stacked plates

Figure 1 Plate geometry illustration

Figure 2a shows a unitary cell of the PHE passages, and surface contact at the corners can be clearly seen. The parameters of corrugation is illustrates in Figure 2b. It is completely specified by the corrugation pith P=15 mm, internal height H=5 mm, inclination angle β=90°, the length of the plate L_p=500 mm and the width of the plate W_p= 500 mm. The most common definition of equivalent diameter is D_e = 2·H = 10 mm.

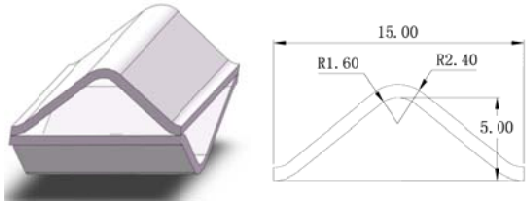

(a)Unitary cell (b) Corrugation profile

Figure 2 Unitary cell and corrugation profile

Figure 3 shows the computational domain which can be divided into five parts:

(1) R1: inlet extended region, length $L1$=1.5L_p;

(2) R2: transition region, length $L2$=0.5L_p;

(3) R3: corrugated plate region, length $L3$= L_p;

(4) R4: transition region, length $L4$=0.5L_p;

(5) R5: outlet extended region, length $L5$=4.5L_p。

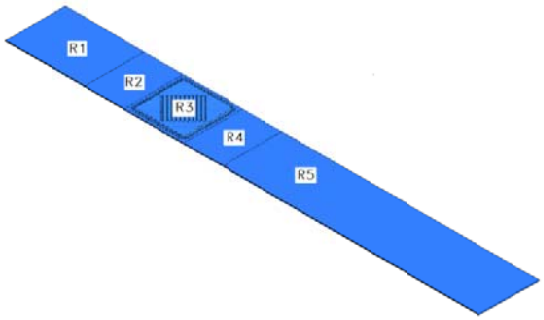

Figure 3 Computational domain

Mesh Generation

The commercial software ANSYS ICEM is used to generate the required meshes. For the irregular passage, it is difficult to divide the zone to generate grids separately. The mesh must be generated through the whole zone one time.

Meanwhile, it is difficult to generate unstructured grids around the contact points. So many contact points always make the mesh generating process hard and inefficient. To avoid the warping of the normal directions during boundary meshing, it is critical to generate good-quality, high-aspect-ratio cells.

A new approach is proposed to overcome such difficulties. A tiny clearance c between two adjacent plates is given to improve the mesh performance around the contact points. If the clearance is too small, the mesh generating process easily divergence and introduces error. If the clearance is too big, the

accuracy of the CFD results is low. In this paper, comprehensive efforts are paid for defining the scale of clearance. At last, a clearance c varying between 0.0 mm~0.6 mm is studied. The results are shown in the next section.

The mesh interval is 0.5 mm in the corrugated plate region R3, 1.0 mm in the transition region R2 and R4, and 5.0 mm in inlet extended region R1 and outlet extended region R5. The mesh method is OCTREE (details can be found in reference [12]), and the mesh type is Tetrahedron. The OCTREE mesh method is based on the following spatial subdivision algorithm. The algorithm ensures refinement of the mesh where necessary, but maintains large element where possible, allowing faster computation. Once the "root" tetrahedron, which enclose the entire geometry, has been initialized, tetra subdivides the root tetrahedron until all element size requirements are met. A tetrahedron has 4 vertices, 6 edges, and is bounded by 4 triangular faces.

Fluent Solves Setup

In the FLUENT solves, the setup of boundary conditions and turbulence model is very important.

(1) In the upstream region. The upstream region includes two parts: the inlet extended region R1 and transition region R2. The velocity and temperature are constant at the inlet boundary. In all the simulations, the inlet temperature is 300K. Velocity-inlet boundary conditions are applied to the inlet boundary and wall boundary conditions are applied on the side boundaries. The thermal boundary on the wall is set as a heat flux of 0 W/m^2. It means that the fluid flows in upstream region without heat transfer. The heat transfer happens just in the plate region.

(2) In the downstream extended region. The downstream region includes two parts: the outlet extended region R5 and transition region R4. For all the variables the stream-wise gradients are set to zero at the outlet boundary named outflow boundary condition. Wall boundary conditions are applied to the side boundaries. The thermal boundary on the wall is set as a heat flux of 0 W/m^2. It means that the fluid flows in downstream region without heat transfer. The heat transfer happens just in the plate region.

(3) In the plate region R3. Wall boundary conditions are applied to the boundaries. A constant temperature of 330K is defined on the plate surface region.

(4) Turbulence model. The Realizable k-ε model is adopted and the near wall treatment uses the enhanced wall treatment. This choice based on previous experience.

(5) Water is the fluid with constant properties at the temperature of 273.15K.

RESULTS AND DISCUSSION

The Comparison of Different Clearances c/D_e

During the optimization of a PHE using CFD, the problem of how to create a high-quality mesh inside complex and irregular channels is important. The reason is that low-quality meshes are easily inducing divergence in the computational process and the process is terminated.

In ICEM, the mesh quality for Tetra element equals to aspect ratio [12]. The definition of the aspect ratio for a Tetra element is [12]:

$$\text{Aspect ratio} = \frac{(\text{volume}/(\text{circumscribed radius})^3)_{\text{actual}}}{(\text{volume}/(\text{circumscribed radius})^3)_{\text{ideal}}}$$

The values are scaled, so that an aspect ratio of unity corresponds to a perfectly regular element, while an aspect ratio of zero indicates that the element has a zero volume (a flat tetra). Refining the surface mesh size or increasing the offset distance will help to increase the aspect ratio. In this paper, to improve the mesh quality around the contact points of two adjacent corrugated plates, a new approach providing a proper clearance between two adjacent plates is studied.

After mesh generation, the computational cell number N_c is about 67 million. Figure 5 shows a shell mesh and a volume mesh by tetrahedron.

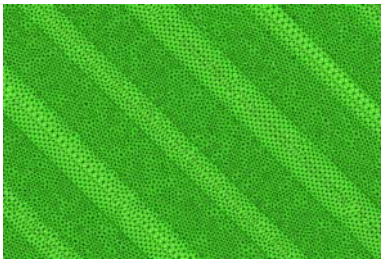

(a) Shell mesh display

(b) Volume mesh display

Figure 5 Mesh display

Figure 6 illustrates the histogram of the mesh quality for tetrahedron elements. In the figure, the horizontal axis represents mesh quality q (equals aspect ratio for tetrahedron) and the vertical axis represents the computational cell number N_c, separately. Different clearance c=0~0.6 mm are studied. For c/D_e=0, it can be seen the lowest mesh quality less than 0.05 and there are many cells whose quality below 0.3. For c/D_e=0.02, the lowest mesh quality is above 0.3. For c/D_e=0.04, the lowest mesh quality is above 0.4. For c/D_e=0.06, the mesh quality is almost above 0.5. From this comparison, it can be seen that as the clearance is increased, the mesh quality is obviously upgraded and also the number of poor cells is greatly decreased.

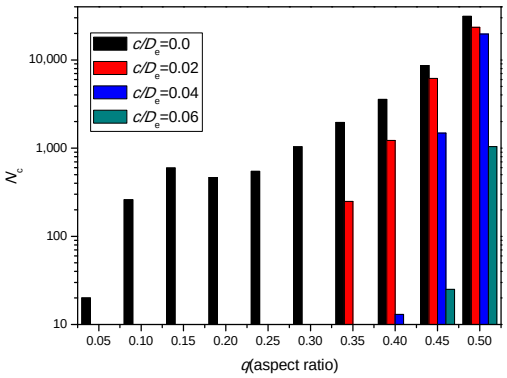

Figure 6 The histogram of mesh quality

Although the clearance is favorable to improve the mesh quality, the influence of such treatment on the results also needs to be investigated. Careful work has been done and the results are shown in Figure 7 and Figure 8. Figure 7 shows the comparison of the heat transfer coefficient h for different c/D_e. It can be seen the results of c/D_e=0.02 agree well with those of c/D_e=0.0. However, that a large deviation occurs compared to c/D_e=0.04 and c/D_e=0.06. The reason is that due to the increase of clearance, the turbulence induced by the contact point becomes weaker. Meanwhile, as the Re increases from 2000 to 10000, the discrepancy between c/D_e=0.0 and c/D_e=0.06 from 7.5% to 10.1%. The explanation is that as the Re increases, the boundary layer becomes thinner, and the turbulence intensity influenced by contact points becomes more obvious.

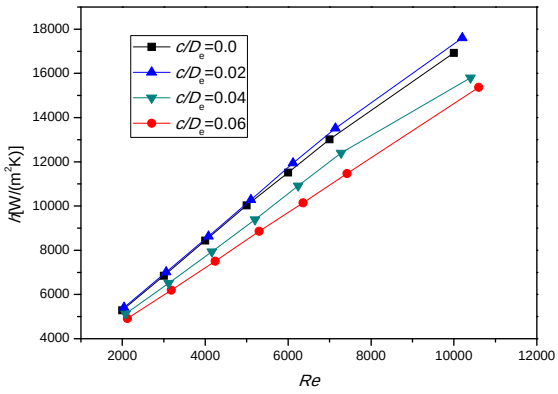

Figure 7 Comparison of h with different c/D_e

Figure 8 shows a comparison of the pressure drop dp for different c/D_e. The dp varies weekly between the cases of c/D_e=0.02 and c/D_e=0.0. Bigger deviation occurs in relation to the cases c/D_e=0.04 and c/D_e=0.06. Furthermore, as the Re increases from 2000 to 10000, the discrepancy between c/D_e=0.0 and c/D_e=0.06 varies from 20.8% to 56.6%. The reason is that the dp is greatly induced by the vortex behind the contact point. At high Re number, the influence of the clearance on the vortex becomes more and more visible, so the deviation is large for a big clearance.

Table 1 gives the detail values of the CFD results as c/D_e=0.02. From the above analysis, the pressure drop is more sensitive than heat transfer as the clearance varies. It can be seen that c/D_e=0.02 is a proper clearance which ensures the computational accuracy as well as it improves the mesh quality obviously. Actually, in engineering, the clearance between two adjacent plates may occur in two cases. First case, for a cold-pressed plate, the spring-back of the corrugations is not uniform. When plates are stacked, local areas of clearances without contact points may exist. The Chinese standard of plate heat exchangers [13] gives the allowable deviations between actual and ideal of corrugation heights. For example, when the plate area $A \leq 0.3\text{m}^2$, this deviation value is $\pm$0.1mm. The other case, because a pressure difference exists between hot and cold fluids, the passage with high-pressure will expanded with no-contact points, and the passage with a low-pressure will be compressed.

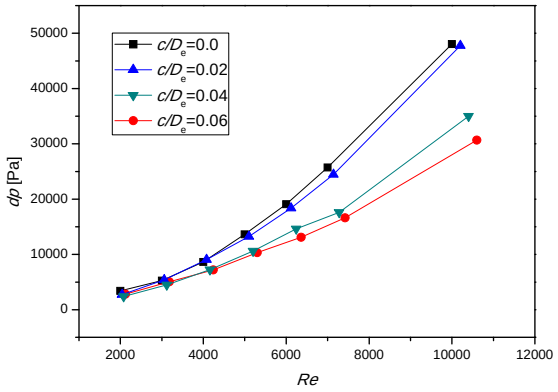

Figure 8 Comparison of dp with different clearance c/D_e

Table 1 CFD results for c/D_e=0.02

V_{in}, m/s	Re	Q, kW	LMTD, K	h, kW/(m^{2}K)	dp, kPa
0.2	2040	71.9	20.9	5.41	2.74
0.3	3060	97.6	22.0	7.01	5.42
0.4	4080	122	22.5	8.62	9.05
0.5	5100	148	22.7	10.2	13.26
0.6	6120	173	22.9	11.9	18.37
0.7	7140	198	23.1	13.5	24.63
1.0	10200	262	23.5	17.6	47.75

Fluid Flow and Thermal Analysis

Figure 9 shows the streamlines in the PHE for the inlet velocity 0.4 m/s and Re=4080. It can be seen that the flow distribution is uniform and the fluid flows through the passage like a zig-zag and net-type route. In the large-view, the blank zones responsent the contact points, and the flow pattern is clearly illustrated near the contact points.

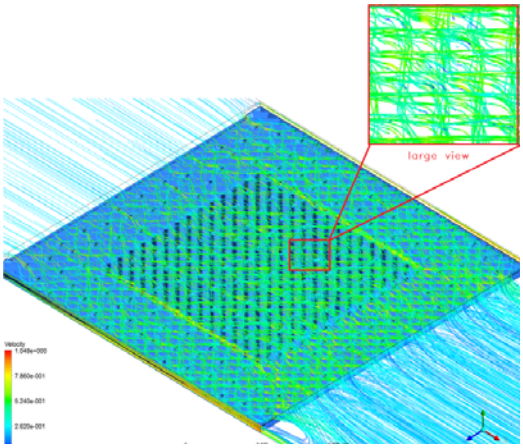

Figure 9 Streamline

Figure 10 illustrates the velocity vectors around the contact points. It shows that there exist small vortices behind the contact points. The mechanism can be explained similar to the flow around the bluff bodies. The fluid flow in the passage is interrupted by many contact points so that the turbulence is intensive and the heat transfer coefficient is greatly upgraded.

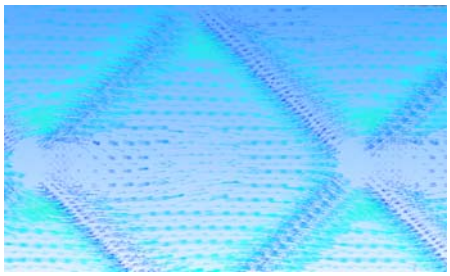

Figure 10 Velocity vectors around the contact points

Figure 11 shows the static pressure distribution. The value is decreased for the reason of friction resistance. The pressure is uniform perpendicular to the main flow direction, and continues to decrease in the main flow direction.

Figure 12 shows the temperature distribution. Similar conclusions can be drawn as for the pressure distribution. The flow is uniform in every separate passage. Complex flow and temperature fields are established in the cross-corrugated passage, which may result in high wall-fluid heat transfer rates.

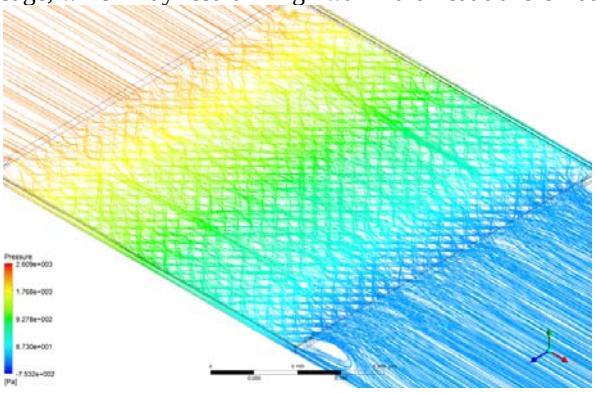

Figure 11 Pressure distribution

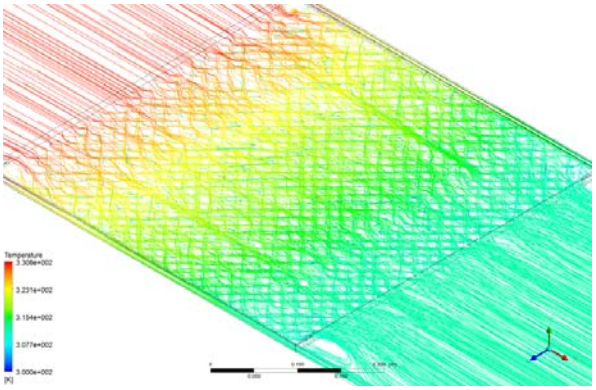

Figure 12 Temperature distribution

Validation of the CFD Results by Experiments

An experimental work was conducted to validate the CFD results for c/D_e=0.02. Due to the limitation of paper length, the experimental is referred to the previous work [10].

The PHE prototype is tested by the experimental system mentioned above. The heat transfer j factor is defined by[14]:

$$j = NuPr^{-\frac{1}{3}}\left(\frac{\mu}{\mu_w}\right)^{-0.17} \quad (2)$$

where Nu is the Nusselt number, Pr is the Prandtl number and μ is the dynamic viscosity.

The correlations of the experimental results and CFD results are fitted separately as below. There can be useful for the design and rating of PHEs.

$$j = 0.236Re^{0.684} \quad (3)$$

$$j = 0.302Re^{0.645} \quad (4)$$

Figure 13 shows a comparison of the CFD and experimental results (10% error bar). It was found that the errors between CFD and experimental results are controlled with ±10% in the Re ranges from 1000 to 7000.

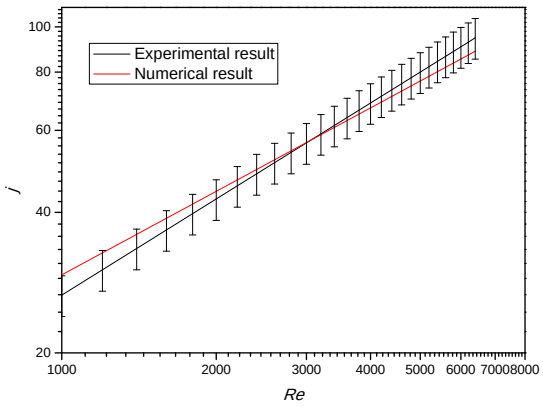

Figure 13 Comparison of CFD and experimental results (10% error bar)

CONCLUSIONS

The paper proposes a new approach to improve the mesh quality of corrugated passages. Many validation works has been done. With the approach, a user can upgrade the mesh quality greatly as well as decrease the low-quality cell number with minimum effort. The conclusions can be summarized as:

(1) The 3D geometry without any simplification is modeled. After mesh generation, the computational cell number N_c is about 67 million. Accompanied with the development of super computers, the CFD can simulate the thermodynamic characters of plate heat exchanger in a large scale and more realistic computational domains.

(2) A tiny clearance c between two adjacent corrugated plates is given to improve the mesh performance around the contact points. For $c/D_e \geq 0.02$, the lowest mesh quality is above 0.3.

(3) The discrepancy between c/D_e=0.0 and c/D_e=0.06 is studied. As the *Re* increases from 2000 to 10000, the deviation of h varies from 7.5% to 10.1% and the deviation of dp varies from 20.8% to 56.6%, respectively. The value of the pressure drop is more sensitive than the value of heat transfer as the clearance varies.

(4) According to massive validation works, the c/D_e=0.02 is found to be a proper clearance which ensures the computational accuracy as well as improvement the mesh quality.

(5) The error between CFD and experimental results can be controlled within ±10% in the *Re* ranges from 1000 to 7000.

This approach is promising and practical but needs further investigation and optimization.

ACKNOWLEDGEMENT

The project is funded by China Postdoctoral Science Foundation, Shanghai Rising-Star Program, the Swedish Research Council (VR) and the Swedish Energy Agency.

REFERENCES

[1] Abu-Khade M.M., Plate heat exchangers: Recent advances, *Renewable and Sustainable Energy Reviews*, Vol. 16, 2012, pp.1883-1991

[2] Luan H. B., Tao, W. Q., Zhu, G. Q., Chen B., and Wang S., Recent advances of all-welded plate heat exchanger, *Sci. China Tech Sci.*, Vol. 43, No. 9, 2013, pp1020-1033

[3] Tao, W. Q., Numerical Heat Transfer (2nd Edition), Xi'an: *Xi'an Jiaotong University Press*, 2001, (In Chinese)

[4] Sunden B., Computational fluid dynamics in research in design of heat exchangers, *Heat Transfer Engineering*, Vol. 28, No. 11, 2007, pp. 898-910

[5] Bhutta M.M.A., Hayat N., Bashir M. H., Khan A. R., Ahmad K. N., and Khan S., CFD applications in various heat exchangers design: a review. *Applied Thermal Engineering*, Vol. 32, 2012, pp.1-12.

[6] Bouriver L., Moreau A., and Ronse G., Six T., Petit J. and Delaplace G., A CFD model as a tool to simulate β-lactoglobulin heat-induced denaturation and aggregation in a plate heat exchanger, *Journal of Food Engineering*, Vol. 136, 2014, pp. 56-63

[7]Han X.H., Cui L.Q., Chen S. J., Chen G. M., and Wang Q., A numerical and experimental study of chevron corrugated plate heat exchanger, *International Communications in heat and mass transfer*, Vol. 37, 2010, pp. 1008-1014.

[8] Gherasim I.L., Taws M., Galanis N., and Nguyen C. T., Numerical and experimental investigation of buoyancy effects in a plate heat exchanger, *Applied Thermal Engineering*,Vol. 51, 2013, pp347-363

[9]Tiwari A.K., Ghosh P., Sarkar J., Dahiya H. and Parekh J., Numerical investigation of heat transfer and fluid flow in plate heat exchanger using nanofluids, *International Journal of Thermal Science*, Vol. 85, 2014, pp.94-103

[10]Luan H.B., Tao W.Q., Zhu G.Q., Chen B. and Wang S., Numerical simulation of complicated chevron plate passages, *Proceedings of the 15th International Heat Transfer Conference*, Japan, August 2014

[11]Giugiu O., Plesa A., and Socaciu L., Plate heat exchangers-flow analysis through mini channels, *Energy Procedia*, Vol 85, 2016, pp.244-251

[12] Documentation for ANSYS ICEM CFD 13.0, ANSYS INC., 2010

[13] China National Energy Administration, Plate heat exchanger, NB/T 47004-2009, Chinese Standard

[14] HTRI design manual, Heat Transfer Research, Inc., 2013, p. B3.1-22.